Testing isotherm models and recovering empirical relationships for adsorption in microporous carbons using virtual carbon models and grand canonical Monte Carlo simulations

2008 J. Phys.: Condens. Matter 20 385212

(http://iopscience.iop.org/0953-8984/20/38/385212)

IOP Publishing Journal of Physics: Condensed Matter

J. Phys.: Condens. Matter **20** (2008) 385212 (15pp) doi:10.1088/0953-8984/20/38/385212

Testing isotherm models and recovering empirical relationships for adsorption in microporous carbons using virtual carbon models and grand canonical Monte Carlo simulations

Artur P Terzyk[1,4,5], Sylwester Furmaniak[1], Piotr A Gauden[1], Peter J F Harris[2,4,6] and Jerzy Włoch[3]

[1] Department of Chemistry, Physicochemistry of Carbon Materials Research Group, N Copernicus University, Gagarin Street 7, 87-100 Toruń, Poland

[2] Centre for Advanced Microscopy, University of Reading, Whiteknights, Reading RG6 6AF, UK

[3] Department of Chemistry, Synthesis and Modification of Carbon Materials Research Group, N Copernicus University, Gagarin Street 7, 87-100 Toruń, Poland

E-mail: aterzyk@chem.uni.torun.pl and p.j.f.harris@rdg.ac.uk

Received 2 June 2008, in final form 5 August 2008
Published 27 August 2008
Online at stacks.iop.org/JPhysCM/20/385212

Abstract

Using the plausible model of activated carbon proposed by Harris and co-workers and grand canonical Monte Carlo simulations, we study the applicability of standard methods for describing adsorption data on microporous carbons widely used in adsorption science. Two carbon structures are studied, one with a small distribution of micropores in the range up to 1 nm, and the other with micropores covering a wide range of porosity. For both structures, adsorption isotherms of noble gases (from Ne to Xe), carbon tetrachloride and benzene are simulated. The data obtained are considered in terms of Dubinin–Radushkevich plots. Moreover, for benzene and carbon tetrachloride the temperature invariance of the characteristic curve is also studied. We show that using simulated data some empirical relationships obtained from experiment can be successfully recovered. Next we test the applicability of Dubinin's related models including the Dubinin–Izotova, Dubinin–Radushkevich–Stoeckli, and Jaroniec–Choma equations. The results obtained demonstrate the limits and applications of the models studied in the field of carbon porosity characterization.

S Supplementary data are available from stacks.iop.org/JPhysCM/20/385212

M This article features online multimedia enhancements

(Some figures in this article are in colour only in the electronic version)

1. Introduction and the aims of the study

One of the most important advantages of molecular simulations is the possibility of testing different theoretical models and approaches. In the field of physical adsorption on porous carbons many new possibilities are offered by so called 'virtual porous carbons' (VPC) as was pointed out by Biggs *et al* [1–3]. Using different VPC models one can test the fundamental ideas applied for many years, for example the BET concept of surface area [4, 5], different isotherm models (for example the IAS approach [6], DR and DA equations [7, 5]) the

[4] Authors to whom any correspondence should be addressed.

[5] http://www.chem.uni.torun.pl/~aterzyk/

[6] http://www.personal.rdg.ac.uk/~scsharip/pjfhhome.htm

idea of α_s plots [4, 5], fractal analysis [8] and adsorption potential distribution [9], and so on. However, for activated carbons many simulations have been performed based on the idealized carbon slit pore model, which seems to be far from reality [10–12]. Moreover, the application of the global adsorption isotherm equation and calculating the global isotherm as the sum of adsorption in individual (usually ideal) slit-like pores do not take into account many different and important factors affecting the mechanism of adsorption, for example pore connectivity.

In this study we use GCMC simulations for the adsorption of different molecules (and at different temperatures) on carbon models proposed by Harris *et al* [9, 13–16]. There are two major aims of this research. The first is to test the Dubinin-related approaches. The second is to show that different empirical correlations reported previously from adsorption data measured on activated carbons can be successfully recovered by simulations, and that this gives a deep insight into their origin on a molecular level.

For adsorption in microporous carbons the Dubinin model has been widely applied, and has made a great contribution to surface science [17]. For example Linares-Solano *et al* applied this model for the determination of microporosity evaluation of activated carbons with burn-off [18] and Carrasco-Martin *et al* showed the linearization of the DR-plots for adsorption of nitrogen and carbon dioxide on a series of Spanish bituminous coals [19]. It was also shown that the parameter n of this equation decreases with burn-off [20]. Kakei *et al* [21] studied nitrogen adsorption on ACFs having slit-like pores. They showed that the DR-plot can be divided into four ranges of linearity called L, M, H, and S. In the L region ($\ln^2(p_0/p)$) $<$ ca 30 nitrogen molecules fill bi-layer sized pores of the highest adsorption potential. After bi-layer filling there is monolayer adsorption of molecules in three and four-layer sized pores, which is observed in the M region ($15 < \ln^2(p_0/p)) < 30$. Molecules in the H region fill the gaps between micropore walls that are coated by monolayers (cooperative process). Finally in the S region adsorption on external surface occurs (note that the general classification of the DR-plots was given by Marsh and Randt [22]). Ozawa *et al* proposed the generalization of the DA model and its application to the description of sorption data of supercritical gases on molecular sieving carbon [23], and from that time the model has also been applied to description of supercritical adsorption. The linearization of the DR-plots was proved, for example, for adsorption data of alkanes on activated carbons [24] and for adsorption of sub and supercritical Xe in micropores of ACFs [25]. This model (and modifications) is also applicable for a description of adsorption from solutions [26], for a description of mixed gas adsorption [27] or excess isotherms [28]. The model is still being modified and has been the subject of many theoretical studies. Jaroniec [29] derived the DR equation from statistical thermodynamics showing that this is a special case of an exponential isotherm. A similar approach was proposed by Ustinov *et al* [30], who studied the statistical analogue of the DA equation. Their approach explained why the overall integral energy of adsorbed molecules grows in spite of an increase in the molecular interactions with increasing adsorption. Chen and Yang [31, 32] showed that in the moderate coverage region there exists a simple inverse proportionality between the characteristic energy and pore diameter. For pores having sizes in the range 1–2 times larger than the diameter of the adsorbate molecule different potential average schemes yield very close values of the mean field indicating that the average scheme is not important in this case. Therefore, the validity of the DR model is confirmed since different microporous materials of practical importance have pores of these dimensions. Dobrushkin [33] concluded that the DA equation is a special case of the approach derived from the condensation approximation. The parameter n is related to the dispersion of pores and does not depend on pore dimension, in this way it characterizes the surface heterogeneity (the more surface is heterogeneous the smaller n is). The second heterogeneity parameter is E_0. The relationships between both parameters of the DA equation and the average pore diameter were proposed recently [34–36]. Some studies on the properties of DA equation were also performed by us [37].

Dubinin's approach was modified to take into account the compressibility of the adsorbate in the calculation of pore volumes [38]. Some theoretical studies also point out that the state of adsorbate molecules in micropores is different from that of the molecules in bulk [39]. The critical temperatures in micropores is much lower than in the bulk, so micropore filling cannot be identified with bulk condensation. Thus p_0 cannot be generally identified with the saturated vapour pressure value. This idea was successfully developed [40] and the applicability of proposed model to a description of adsorption data of supercritical gases on carbons was proven. This was also confirmed by Tovbin [41] who derived equations analogous to the DR model; however, the saturated vapour pressure was replaced by p.

The properties of Dubinin model have also been studied by molecular simulations. For example Samios *et al* [42] showed a good fit between average pore diameter of carbon calculated from the DR equation and from simulated adsorption isotherms of CO_2. Ohba *et al* [43], simulated nitrogen adsorption local isotherms in slits having different widths, assumed a Gaussian distribution of pores, and constructed DR-plots. They noted that all DR-plots had a brief linear range below $\ln^2(p_0/p) = 60$, but deviated downward at higher values. This deviation was previously assigned to insufficient diffusion but now they concluded that it comes from the submonolayer adsorption on pore walls. A linear DR-plot corresponds to the micropore filling range. They also confirmed the goodness of the Dubinin–Stoeckli relation. The same group [44] presented an extension of the above mentioned concept to different versions of the PSDs (also asymmetric), and also performed simulations for different temperatures. The deficient pore width distribution in the small pore width range shifts the DR-plot downward. At the same time the stepwise structure in the low relative pressures range disappears by due to the lack of small pores. On the other hand, the excess pore width distribution in the small pore width range shifts the DR-plots upward. Therefore, the stepwise structure in the simulated DR-plot stems from the adsorption jump in narrow pores.

El-Merraouni *et al* [45] showed a comparison of PSDs of activated carbon fibres using NLDFT, and Dubinin–Stoeckli method. DFT PSDs were usually bimodal with sharp peak located at 0.6 nm and a broad peak at larger pore widths. The separation of both peaks increased for larger pore size samples. The lowest peak from the DFT was absent in the DS distribution (the latter assumes one modal Gaussian function). Nguyen and Do [46] concluded that for applicability of DR model solid must have a distribution of micropores, and this distribution must not be much skewed. Therefore, DR is not applicable to all microporous materials. The study performed by Aranovich and Donohue [47] pointed out the defects of the DR equation. In particular the derivation of this equation is based on the arbitrary assumption that there is a Gaussian distribution of adsorption space with respect to the adsorption potential; moreover, the energetic parameter of this equation is not clearly defined. Moreover, DR does not reduce to the Henry's law limit. Nevertheless, this equation and its modifications have been used for 60 years for the analysis of vapour adsorption on microporous adsorbents with I type of isotherms.

The observations given above validate further studies of the Dubinin–Astakhov and related approaches, as presented in this paper. As mentioned by Ohba and Kaneko '*still the DR equation must be studied from a different angle*' [44]. Therefore, the results of our previous study [9] are extended to the adsorption of different adsorbates and for some cases on adsorption at different temperatures. To our knowledge, this is the first report showing the comparative DR-type analysis of sorption of different adsorbates using the simulation technique and VPC. We are also interested in investigating the validity of the so called temperature invariance of the characteristic curve (TICC). This is an important and rarely studied issue. Thus, for example, Dubinin and Astakhov [48] showed the validity of TICC for C_6H_6 adsorption on Saran carbon. Nakahara *et al* [49] proved the validity of DA model and the TICC for adsorption of hydrocarbons on carbon molecular sieves. On the other hand, Zukal and Kadlec [50] recorded the deviation from the TICC for ethanol adsorption on Desorex carbon, explained by different degrees of association in liquid and vapour phases. Different results were obtained by Lopez-Ramon *et al* [51] who showed that TICC is fulfilled for the adsorption of alcohols on carbons. The validity of TICC was brought into question by the data of Pons and Grenier [52] for the adsorption of alcohols on carbons. Bakaev and Steele [53] published a detailed review on TICC and concluded that TICC is a result of the fact that the entropy of physical adsorption is close to (and slightly less than) the entropy of a bulk liquid, because the heat of physical adsorption is close to (and slightly higher than) the heat of condensation. Therefore, TICC reflects the occurrence of so called Barclay-Butler relationship widely observed in physical chemistry [54].

Since in simulations the structure of an adsorbent can be prepared in such a way that the porosity is known, it is possible to check the influence of porosity and the nature of adsorbed molecules on TICC. In the current study we will try to check this for two nonpolar adsorbates, namely benzene and carbon tetrachloride. Moreover, we will verify the applicability of Dubinin–Izotova model [55] (proposed as a consequence of deviation of DR-plots from linearity [56] and successfully applied for characterization of glassy carbons [57]), Dubinin–Radushkevich–Stoeckli [58] and Jaroniec–Choma [59] approaches. For reviews dealing with the models mentioned see [60, 61].

2. Carbon models

Two models of microporous carbons were applied, called **S0** and **S35**. The origin of the models was given previously [9, 16]. A comparison of both structures is shown in figure 1 where we also present the pore size distribution curves obtained using the Bhattacharya and Gubbins (BG) method [62] previously tested and applied successfully for different virtual porous carbons [9, 16]. It should be noted that this figure and two movies attached to supplementary data (available at stacks.iop.org/JPhysCM/20/385212) were created using the VMD program [63].

3. GCMC simulations

We applied the GCMC method in the following way. Adsorption of noble gases was simulated for the temperature of boiling (for Ne, Ar, Kr and Xe: 27, 87, 119.93 and 165 K, respectively) for **S0** and **S35** VPCs, and graphite. To study the TICC, adsorption of CCl_4 and C_6H_6 was simulated for 288, 298 and 308 K for **S0** and **S35** VPCs and for the middle temperature for graphite.

Periodic boundary conditions were applied in all three directions. The dimensions of simulation boxes were the same for all structures (4.6 nm × 4.6 nm × 4.6 nm; 4049 carbon atoms for **S35** and 2704 for **S0**). For each adsorption point 25×10^6 iterations were performed (reaching the equilibrium state), and next 25×10^6 equilibrium iterations (from those results the average values were calculated). Single iteration represents a change of the state of a system *via* displacement, creation, annihilation and rotation of the adsorbate. The probabilities of creation, displacement and annihilation for noble gases were the same (equal to 1/3). For benzene and carbon tetrachloride the probabilities of displacement and rotation were equal to 1/6 (note that the displacement of a molecule in this case is connected with the change in angular position). Noble gases were modelled as Lennard-Jones spheres [9, 16, 64]. Carbon tetrachloride was simulated using the five-centre model [65] where each atom is represented by one LJ centre, assuming the length of carbon chloride bond equal to 0.1766 nm. Benzene was modelled applying the AUA potential, assuming that each CH group of the molecule is represented by single LJ centre and assuming the distance between each united atom as equal to 0.1806 nm [66]. Ungerer *et al* [66] pointed out the very good behaviour of this potential in simulating properties of bulk benzene, and concluded that this potential is physically realistic, as revealed by the reasonable account of the pairwise radial distribution function. Each carbon atom forming the structure of the adsorbents was treated as single LJ centre. The values of the parameters are shown in table 1 (note that the parameters of interactions between different centres

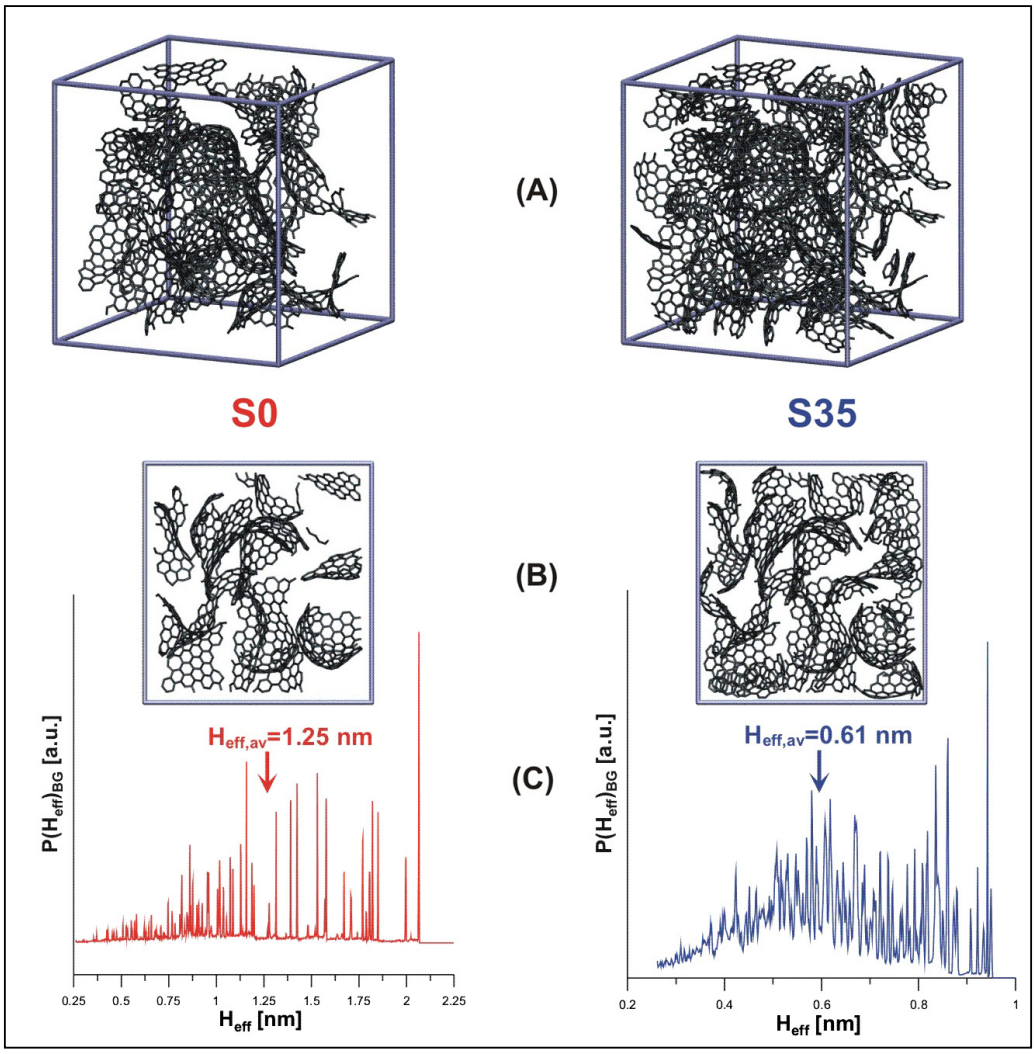

Figure 1. The graphical representation of two studied carbon models. (A) simulation boxes, (B) the boxes seen parallel to surface dividing them into two rectangular prisms, (C) the pore size distributions obtained from BG method (average pore diameters are shown by arrows).

Table 1. The values of the parameters applied in simulations.

Centre	σ (nm)	ε/k_B (K)	Reference
Ne	0.278	34.9	[64]
Ar	0.34	120.0	[9, 16] and the references therein
Kr	0.3685	164.41	[64]
Xe	0.4055	229.0	[64]
		CCl_4	
C	0.46	39.0	[65]
Cl	0.35	105.0	
		Benzene	
ua[a]	0.3246	89.4	[66]
		Carbon structures	
C	0.34	28.0	[9, 16] and the references therein

[a] United atom.

were calculated from Lorentz–Berthelot mixing rule). The enthalpy of adsorption was calculated using the theory of fluctuations [67].

To discuss the influence of the value of the collision diameter, and the values of the LJ potential parameters on the shapes of DR-plots additional simulations were performed. We started from the results of Ne simulation increasing or decreasing the values of ε_{sf}/k_B (11.26, 21.26, **31.26**, and 41.26 K, respectively—here and below the value in bold denotes the starting value for Ne—table 1), ε_{ff}/k_B (14.9, 24.9, **34.9**, 44.9, and 54.9 K, note that in this case the values of ε_{sf}/k_B must be changed, and they were equal to: 20.43, 26.40, **31.26**, 35.46, 42.63 K), and σ_{ff} (0.20, 0.25, **0.278**, 0.30, 0.35, 0.40, 0.45, and 0.50 nm, here also the values of σ_{sf} change and they were equal to: 0.27, 0.295, **0.309**, 0.32, 0.345, 0.37, 0.395, and 0.42 nm, respectively).

To recover the empirical correlation proposed by Stoeckli and Morell [68], it was necessary to simulate the adsorption isotherm and enthalpy of adsorption of studied molecules on graphite. To do this, the simulation box was constructed (4.3959 nm × 4.3005 nm × 6 nm). Graphite was modelled as containing 5 layers (placed in the centre of the box), separated by 0.335 nm (3600 carbon atoms) located in x and y direction. Periodic boundary conditions were applied in three directions,

Table 2. The results of fitting of simulation data on S35 structure by the DR and DA equations. DC—the value of determination coefficient showing the goodness of the fit of model to simulation data.

			DR			DA			
Adsorbate	T (K)	β	a_m (mol g^{-1})	E_0 (kJ mol^{-1})	DC	a_m (mol g^{-1})	E_0 (kJ mol^{-1})	n	DC
Ne	27	0.14	0.045 50	19.69	0.9954	0.045 12	19.33	2.373	0.9986
Ar	87	0.31	0.021 77	17.31	0.9970	0.021 53	17.05	2.429	0.9989
Kr	119.93	0.39	0.016 31	17.29	0.9978	0.016 15	17.16	2.326	0.9990
Xe	165	0.50	0.011 55	17.91	0.9977	0.011 44	17.81	2.326	0.9990
CCl_4	288	1.06	0.004 552	13.11	0.9980	0.004 545	13.08	2.047	0.9981
	298	1.06	0.004 489	13.05	0.9983	0.004 479	13.01	2.056	0.9984
	308	1.06	0.004 429	12.96	0.9989	0.004 429	12.96	2.002	0.9989
C_6H_6	288	1.00	0.005 591	13.62	0.9987	0.005 619	13.70	1.877	0.9989
	298	1.00	0.005 451	13.91	0.9984	0.005 460	13.95	1.956	0.9984
	308	1.00	0.005 432	13.20	0.9980	0.005 502	13.43	1.731	0.9990

and the distance in z direction (effective slit width) was chosen as equal to 4.32 nm, to prevent condensation.

4. Description of simulated results

The fitting of simulation data by the studied models was performed using the genetic algorithm of Storn and Price [69, 70]. All results were described (in the whole pressure range) by a classical Dubinin–Astakhov adsorption isotherm equation, using the values of the affinity coefficient tabulated in the review paper of Wood [71]. Moreover, we applied the Dubinin–Izotova model [55] and the Dubinin–Raduskevich–Stoeckli [58] equation (also in the whole pressure range) in the form [72, 61, 45, 73]:

$$N_{\mathrm{DRS}} = \frac{N_{\mathrm{mDRS}}}{\left(1+\mathrm{erf}\left(\frac{x_0}{\Delta\sqrt{2}}\right)\right)\sqrt{1+2m\Delta^2A_{\mathrm{pot}}^2}} \times \exp\left[-\frac{A_{\mathrm{pot}}^2 m x_0^2}{1+2m\Delta^2A_{\mathrm{pot}}^2}\right] \times\left[1+\mathrm{erf}\left(\frac{x_0}{\Delta\sqrt{2}\sqrt{1+2m\Delta^2A_{\mathrm{pot}}^2}}\right)\right] \quad (1)$$

where N_{DRS} and N_{mDRS} are the values of adsorption and maximum adsorption, respectively, A_{pot} is the adsorption potential, $m = (\beta\kappa)^{-2}$ is a proportional coefficient (κ is assumed as equal to 12 (kJ nm mol^{-1})), β is the similarity coefficient, erf is the error function, Δ and x_0 are 'dispersion' and mean of Gaussian distribution, respectively. The pore size distribution was calculated using the correct normalization factor (i.e. from 0 up to ∞) [72]:

$$\chi_{\mathrm{DRS}}(x) = \chi_{\mathrm{normDRS}}\exp\left[-\frac{(x-x_0)^2}{2\Delta^2}\right] \quad (2)$$

where

$$\chi_{\mathrm{normDRS}} = \frac{2}{\Delta\sqrt{2\pi}\left(1+\mathrm{erf}\left(\frac{x_0}{\Delta\sqrt{2}}\right)\right)}. \quad (3)$$

Finally, the data were also described using the model proposed by Jaroniec and Choma [74–76]:

$$N_{\mathrm{JCh}} = N_{\mathrm{mJCh}}\left[1+\left(\frac{A_{\mathrm{pot}}}{\beta\rho}\right)^n\right]^{-(\nu+1)} \quad (4)$$

where

$$\chi_{\mathrm{JCh}}(x) = \chi_{\mathrm{normJCh}}\exp[-\rho\zeta x^n] \quad (5)$$

and

$$\chi_{\mathrm{normJCh}} = \frac{n(\rho\zeta)^{\nu+1}}{\Gamma(\nu+1)} \quad (6)$$

where Γ is the Euler gamma function, ζ is constant equal to $(1/\kappa^n)$ and ρ, ν, n are the parameters of equations (4)–(6).

The average micropore diameters from DI model were calculated using:

$$H_{\mathrm{eff,av,DI}} = \frac{N_{m1}H_{\mathrm{eff,av1}} + N_{m2}H_{\mathrm{eff,av2}}}{N_{m1}+N_{m2}}. \quad (7)$$

For the remaining models the average micropore diameters were calculated from integration of the PSD curve.

5. Results and discussion

5.1. Adsorption of noble gases

Simulated isotherms, together with the enthalpy of adsorption are shown in figure 2. As for adsorption in typical activated carbons, differences in the shapes of adsorption isotherms are recorded, i.e. isotherms simulated for **S35** structure are sharper, due to narrower PSD curve and smaller diameters of micropores (figure 1). Due to dispersion interactions the isosteric enthalpy of adsorption (q^{st}) values increase with the rise in polarizability of studied adsorbates from Ne up to Xe. For both studied structures, the isotherms obtained follow the Gurvich's rule; thus, the value $(1/\sigma_{\mathrm{ff}}^3)$ correlates linearly with the maximum adsorption determined from simulated isotherms (figure 3). This effect is caused by the differences in volume of pores penetrated by studied adsorbates and also by the packing effect. The results of the description of data for **S35** structure using DR and DA adsorption isotherm equations are collected in table 2. One can observe that for the data simulated for adsorption in this structure there are no remarkable differences between the qualities of the fit for both studied models. For structure **S35** the DA equation recovers maximum adsorption perfectly, and there is the linear correlation between maximum adsorption calculated form the DA equation and this determined from the plateau of isotherms. On the other hand, a poor fit of the DA model was recorded

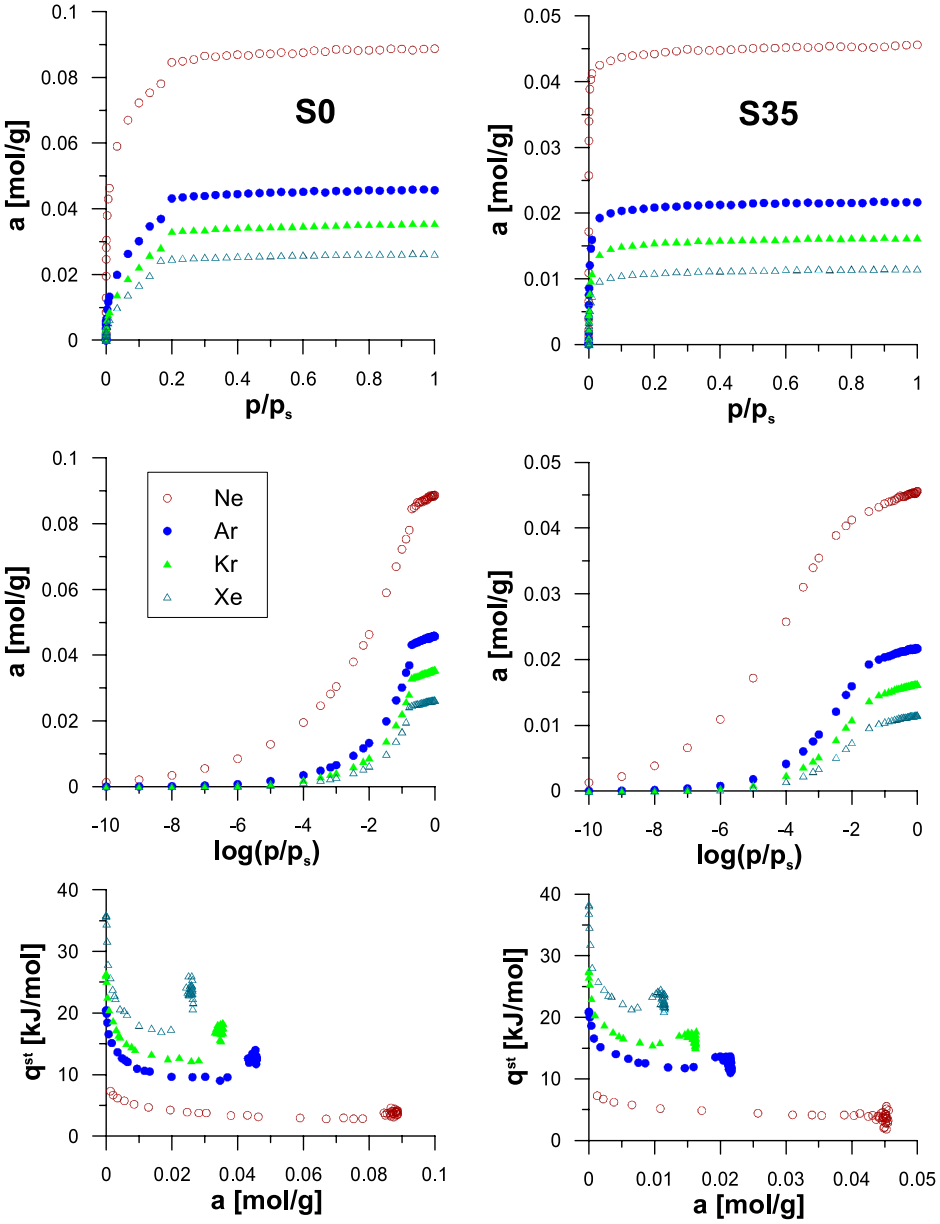

Figure 2. Simulated isotherms and enthalpy of adsorption of noble gases on studied structures.

Table 3. The results of fitting of simulation data on **S0** structure by the DI equation.

Adsorbate	T (K)	β	N_{m1} (mol g^{-1})	N_{m2} (mol g^{-1})	$E_{0,1}$ (kJ mol^{-1})	$E_{0,2}$ (kJ mol^{-1})	n_1	n_2	DC
Ne	27	0.14	0.056 74	0.032 11	14.74	5.562	1.650	2.501	0.9990
Ar	87	0.31	0.025 95	0.019 73	13.77	5.768	1.877	4.286	0.9984
Kr	119.93	0.39	0.020 10	0.015 27	13.80	6.127	1.812	4.739	0.9985
Xe	165	0.50	0.014 63	0.011 59	14.56	6.661	1.942	6.034	0.9983

for the adsorption data on the **S0** structure. Therefore, for this system we firstly applied the Dubinin–Izotova (DI) equation, being the hybrid of two DA models.

The results are collected in table 3, and show good applicability of this model for the studied case. As in the case of the DA model and **S35** structure, one can observe very good linear correlation between the sum of maximum adsorption values calculated from the DI model and the total adsorption from plateau of isotherms. What is also interesting is that the values of maximum adsorption from the DI model on the **S0** structure (N_{m1}, N_{m2} as well as $N_{m1} + N_{m2}$) also correlate very well with $(1/\sigma_{\mathrm{ff}}^3)$. The DR-plots for studied isotherms are collected in figure 4. Generally, they can be divided into even six linear segments

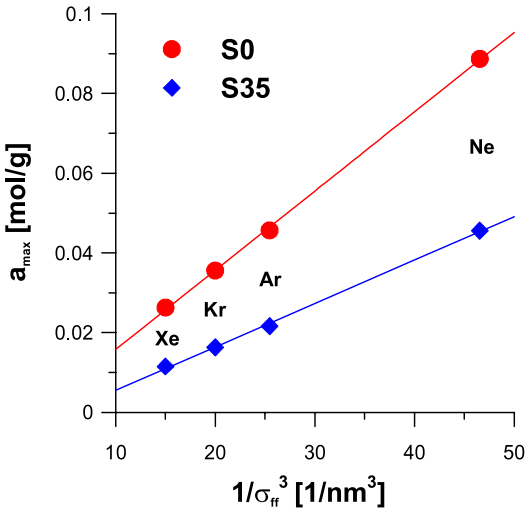

Figure 3. The correlation between $(1/\sigma_{ff}^3)$ and a_{max} from simulation data for studied structures.

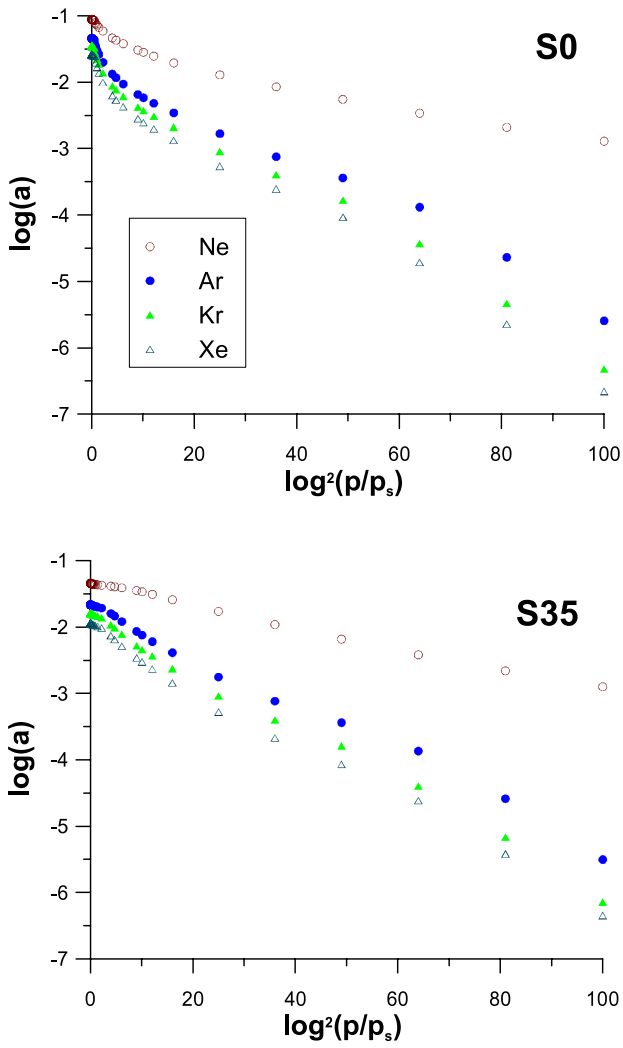

Figure 4. DR-plots of isotherms for noble gases adsorbed on both structures (on y axis data are divided by unitary adsorption).

(in figures S1a and S1b in the supplementary data (available at stacks.iop.org/JPhysCM/20/385212) those plots were shown separately for clarity). The most interesting is Ne adsorption on the **S35** structure, showing only two linear ranges of the DR-plot. Movie 1 from supplementary data (available at stacks.iop.org/JPhysCM/20/385212) shows an animation of the process of adsorption in relation to the obtained DR-plots. One can observe that due to differences in temperature and the collision diameters of Ne and Xe for the first adsorbate the process of filling of pores is more spontaneous and in this case continuous filling of pores is observed. The obtained results also confirm the conclusion of Ohba *et al* [43] that the downward deviation of DR-plots at low pressures (previously assigned to insufficient diffusion) comes from the submonolayer adsorption on pore walls. It is interesting that even for structure **S35** (having narrow distribution of microporosity) deviations on the DR-plots occur for larger molecules, i.e. CCl_4 and C_6H_6 (movie 2, supplementary data (available at stacks.iop.org/JPhysCM/20/385212)). Therefore, one can conclude that the deviations of DR-plots from linearity are caused by the combination of porous structure, packing effects, intermolecular interactions, and collision diameters of adsorbed molecules. The influence of carbon porous structure is visible on DR-plots for data simulated for adsorption in **S0** structure (figure 4). In this case the plot for Ne has at least 4 ranges of linearity, but for larger molecules five or even six. Figures 5–7 show the results of the additional simulations performed to determine the influence of the energy of solid–fluid (ε_{sf}) and fluid–fluid (ε_{ff}) interactions, as well as the value of the collision diameter (σ_{ff}) on the DR-plots. It should be noted that in figures S2–S4 in the supplementary data (available at stacks.iop.org/JPhysCM/20/385212) individual curves are shown separately for clarity. As expected, the decrease in the value of the ε_{sf} (figure 5) changes the shape of the isotherms (note that the maximum capacity is not reached for some cases) but what is more interesting is that the shape of DR-plot changes only for adsorption in **S35** structure, having smaller and not so distributed micropores. The decrease in the value of this energy causes the appearance of small downward deviation at larger pressures, and next this deviation becomes upward for the smallest potential values. The change in the value of the energy of fluid–fluid interactions (in the studied range—figure 6) causes the appearance of downward deviation on DR-plots for the smallest energy value for **S0** structure, but for **S35** structure one can observe the change in the shape, i.e. flattening of the plot for intermediate values, and the appearance of a downward deviation for the smallest value of the energy. Here, especially in the range where those interactions dominate, i.e. in the high pressure limit, changes in the type of deviation (from downward to upward) are recorded, with the decrease in the energy value. For the smallest energy these deviations are noticed also at the intermediate pressures. Finally, in the case of the influence of σ_{ff}, for the **S0** structure the decrease in this value causes the upward deviations to be more visible. A more interesting situation occurs for the **S35** structure, where at small σ_{ff} values an upward deviation occurs; however, the increase in the value of the collision diameter causes the linearization of the DR-plot, although for the largest values one can observe a bimodal DR-plot.

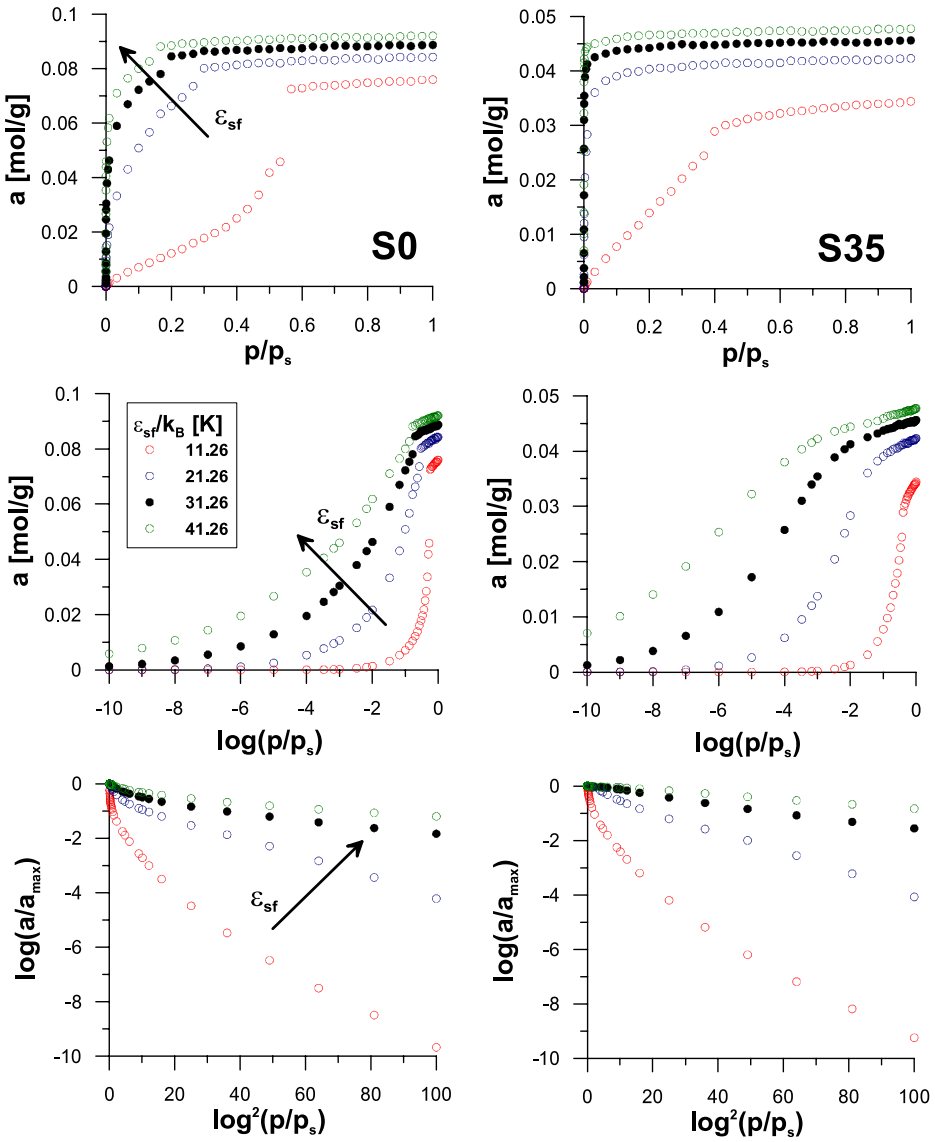

Figure 5. The influence of ε_{sf} ($T = 27$ K; $\sigma_{ff} = 0.278$ nm; $\varepsilon_{ff}/k_B = 34.9$ K) on adsorption isotherms and DR-plots. Black circles show the data for Ne (table 1).

5.2. Adsorption of benzene and carbon tetrachloride

The results of simulations are collected in figures 8 and 9. In this figure we also show the related DR-plots. One can see that due to the rise in temperature, as well as the rise in the collision diameters of both adsorbates (comparing to noble gases) the DR-plots deviate from linearity and five nonlinear fragments are observed.

5.3. Checking the TICC

Figure 10 shows the isotherms of C_6H_6 and CCl_4 and the conversion of both groups of curves into the 'characteristic curves', using the molar volume of liquids at studied temperatures (see figure captions). As one can observe, the TICC is fulfilled for both adsorbates as well as for both structures. Therefore, one can conclude that in the case of adsorption in microporous carbon structures having more (**S0**) or less (**S35**) distributed microporosity, for the case of nonpolar gases as benzene and carbon tetrachloride, TICC is fulfilled. Those results confirm the reality of the studied models, since the TICC was previously observed for carbon tetrachloride adsorption on microporous 'hard' carbon from polyfurfuryl alcohol [77].

5.4. Recovering empirical correlations describing adsorption on microporous carbons from GCMC data

The data obtained can be applied to recovering different correlations widely proposed in the literature. We start from the Cheng and Yang [31, 32] derivation of the DA equation, showing that the characteristic energy of adsorption ($E_0\beta$) is directly related to the mean potential in the pore. Therefore, accepting this derivation, one should expect a relationship between the isosteric enthalpy of adsorption at the zero-coverage limit (q_0^{st}) and the value of ($E_0\beta$). This situation is in fact is observed (figure 11) for data obtained on the

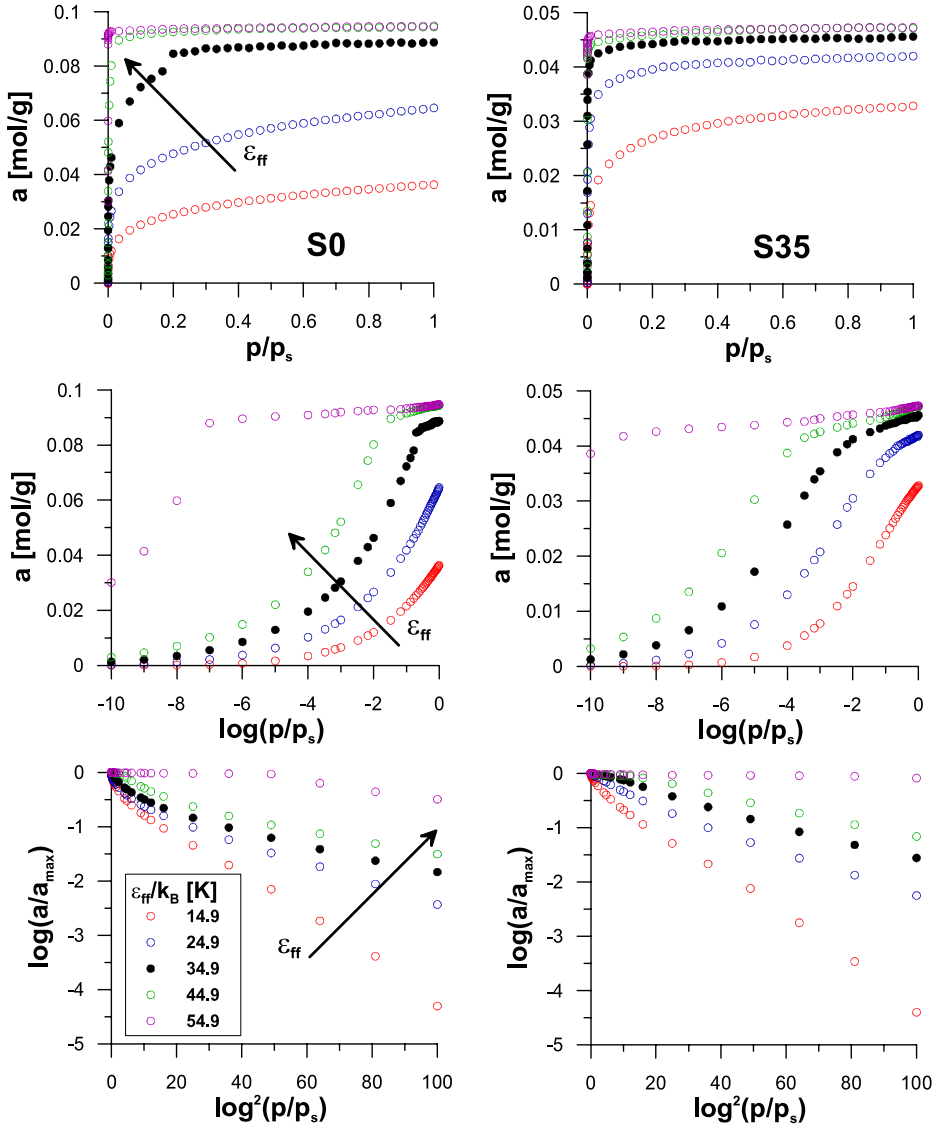

Figure 6. The influence of ε_{ff} ($T = 27$ K; $\sigma_{sf} = 0.3126$ nm) on adsorption isotherms and DR-plots. Black circles show the data for Ne (table 1).

S35 structure. Our obtained results confirm the validity of the postulate of Cheng and Yang showing, that the parameter $(E_0\beta)$ is proportional to the mean potential in the pores.

On the other hand, Stoeckli and Morell [68] using chromatographic data concluded that there is a linear relationship between the difference in energy of adsorption in micropores at zero coverage, and the same energy on graphite, and $(E_0\beta)$ values. Therefore, they showed, that $(E_0\beta)$ represents an average excess of adsorption energy in the micropores, with respect to open graphitic surface. To check this, we plotted the values obtained from simulations on **S35** and on graphite in figure 12, showing very good recovery of this correlation, and confirming the experimental data of those authors. In this figure we show that a more realistic plot (i.e. approaching (0, 0)) is observed if only adsorption of noble gases is considered.

Finally, we checked the relations proposed by Tsunoda [78] who studied many empirical systems showed the relationships between C constant of the BET model and $(E_0\beta)$ from the DR equation. Figure 13 shows that this correlation can be recovered from the results of this study. In fact, Rudziński and Everett [79] derived this relation from theory of adsorption on heterogeneous surfaces.

5.5. Applicability of the DRS and JCh models

Figure 14 shows the applicability of JCh and DRS models to a description of the simulated data. For the **S35** structure both models describe the data with good accuracy (some examples of the fits are shown in figure S5 in the supplementary data (available at stacks.iop.org/JPhysCM/20/385212)); however, for the **S0** structure and for the adsorption of benzene and carbon tetrachloride an insufficient fit was recorded for the JCh model. One can observe good recovery of the absolute BG pore size distribution. What is more important is that the distribution recovered by the models depends on the type of the adsorbate. For the **S0** structure the JCh model works less well

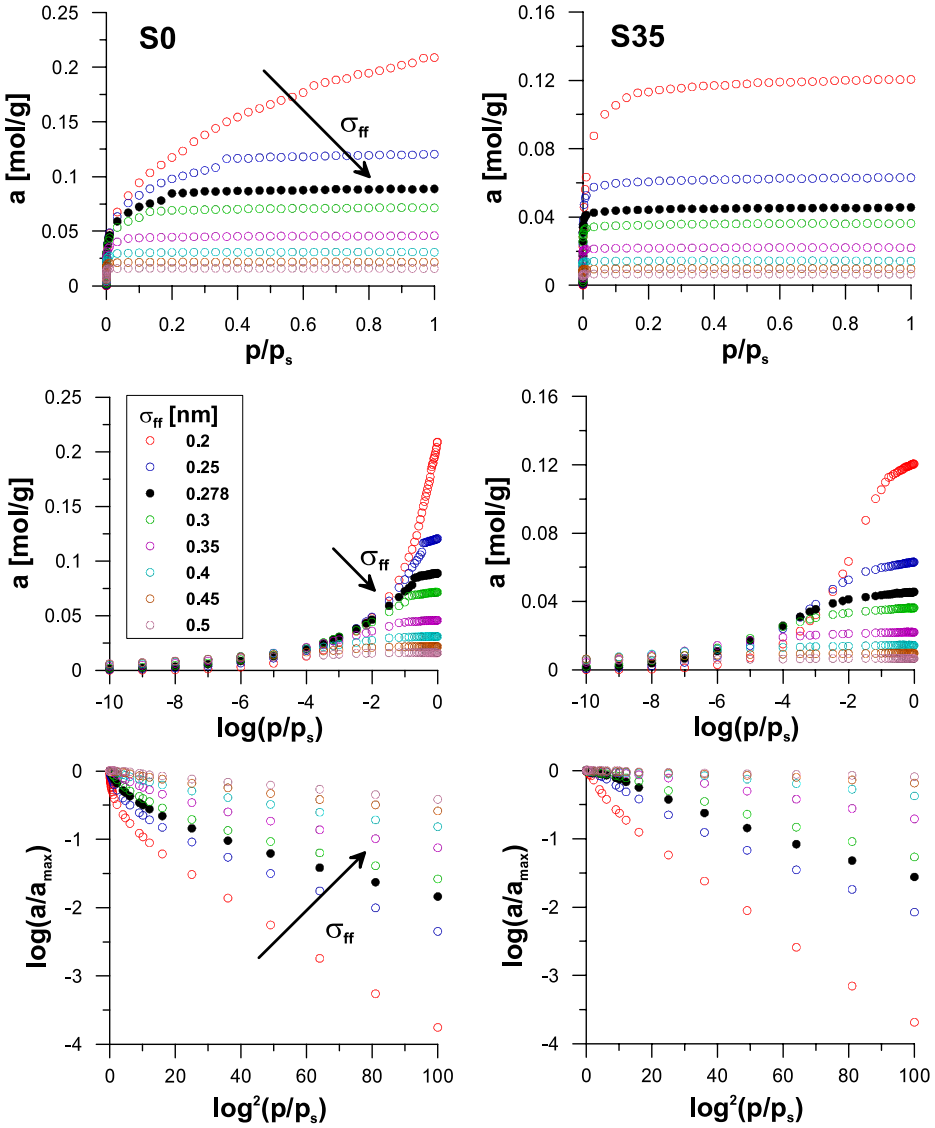

Figure 7. The influence of σ_{ff} ($T = 27$ K; $\varepsilon_{ff}/k_B = 34.9$ K) on adsorption isotherms and DR-plots. Black circles show the data for Ne (table 1).

than the DRS if one compares the shapes of PSDs. Moreover, more realistic shapes and locations of PSDs are shown for the DRS model applied for all studied adsorbates excepting benzene (here the PSD is shifted toward larger micropores). For this structure the JCh distribution is too wide, due to the applied gamma-type model. On the other hand for the **S35** structure the JCh model seems to be more realistic than the DRS (for adsorption of noble gases) and for benzene and carbon tetrachloride the distribution is too wide. The latter effect is also seen on DRS distribution calculated for this structure.

These results are crucial from experimental point of view. One can conclude that if there is a wide distribution of micropores in activated carbon the DRS model leads to the most realistic PSD, and noble gases or carbon tetrachloride adsorption data should be applied to obtain the reliable pore characteristics. On the other hand, if the studied sample is highly microporous, the JCh model should be preferred and one should apply the data of adsorption of noble gases to obtain the most realistic PSD curve.

Finally, the question arises about the reality most important parameter of the structure of activated carbons, i.e. the average micropore diameter. Figure 15 compares the values calculated from the both models for the both studied structures, with the average pore diameter from the BG method. For the structure having distributed microporosity (**S0**) the DRS model predicts the average micropore diameter well, and the best results are recorded for Ar, while for the **S35** structure both models lead to almost the same average micropore diameters, while slightly better results are observed for the DRS model, and for Ne adsorption.

6. Conclusions

We have shown that many empirical correlations can be recovered by GCMC simulations of adsorption on the VPC

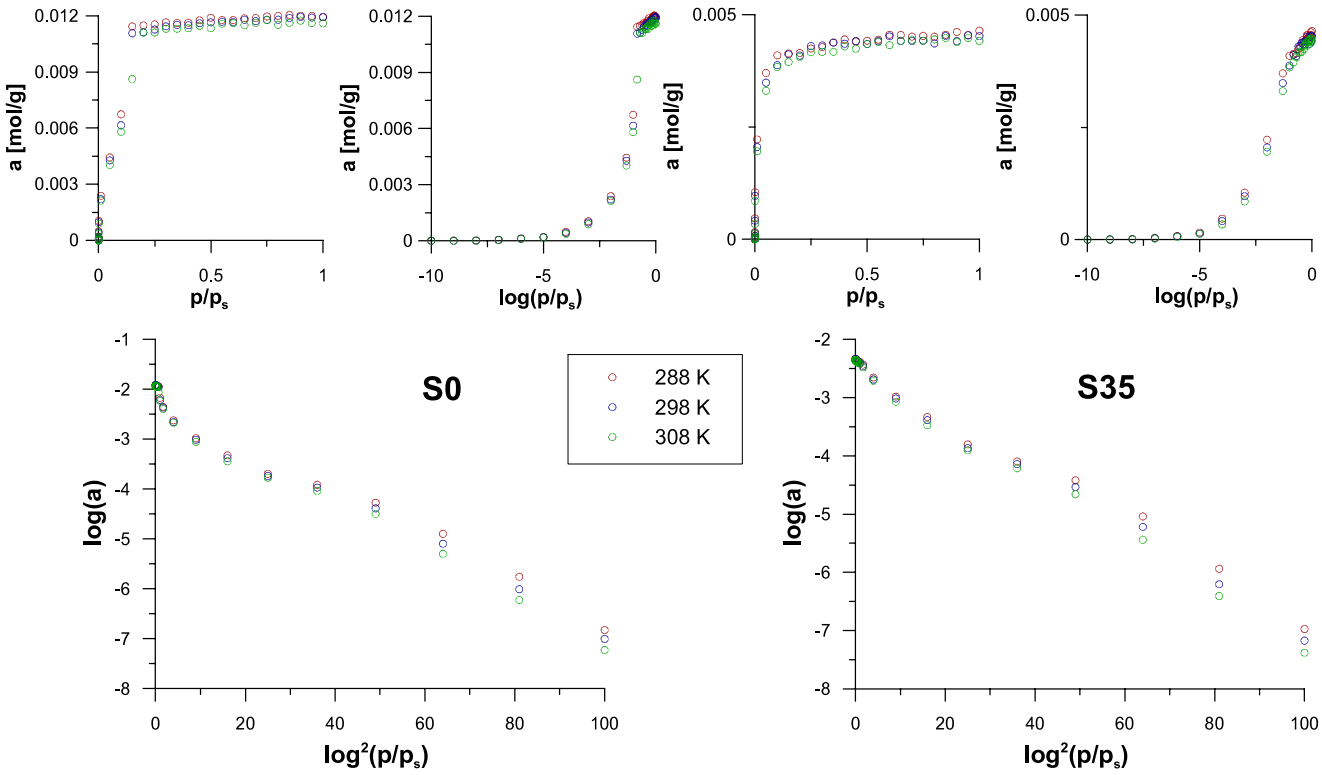

Figure 8. The results of GCMC simulations for CCl_4, and the related DR-plots.

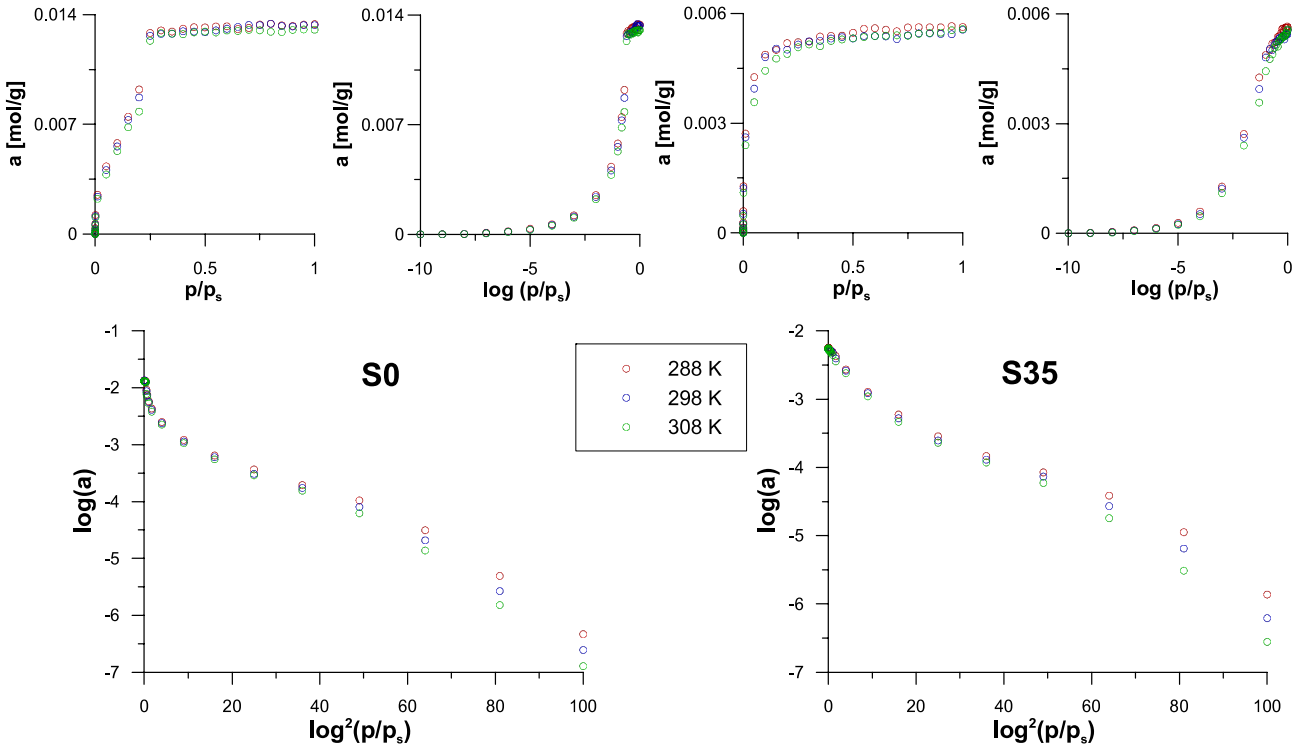

Figure 9. The results of GCMC simulations for C_6H_6, and the related DR-plots.

model proposed by Harris *et al*. Simulation results on the studied models mimic very well the experimental behaviour of real activated carbons fulfilling Gurvich's rule, the empirical correlations developed by Tsunoda or the fundamental relation proposed by Stoeckli and Morell. We have also shown that the validity of the Cheng and Yang derivation of the DA model can be confirmed. The TICC condition is fulfilled for the adsorption of benzene and carbon tetrachloride; therefore, one

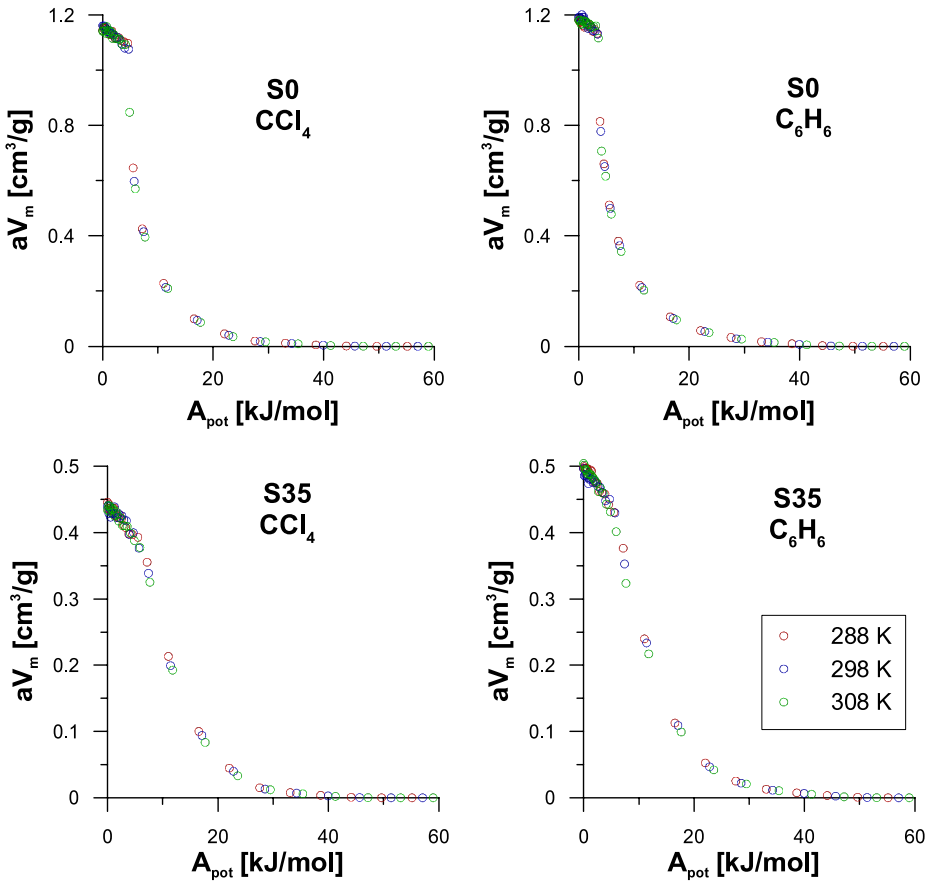

Figure 10. Adsorption isotherms of CCl_4 and C_6H_6 converted into 'characteristic curves'. The following liquid densities ($cm^3\ mol^{-1}$) were used for CCl_4: 95.9628, 97.1688, 98.3748, and for C_6H_6: 88.3493, 89.4435, 90.5376 (at 288, 298 and 308 K, respectively).

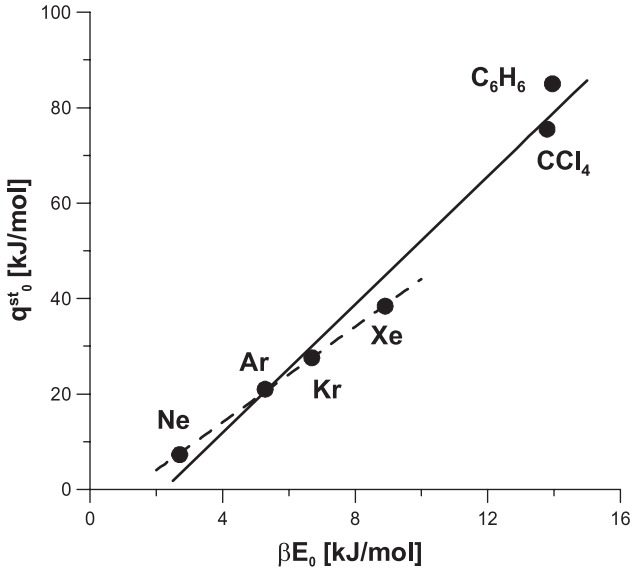

Figure 11. The correlation between βE_0 and the isosteric enthalpy at zero coverage (q_0^{st}) for data on S35 structure; CCl_4 and C_6H_6 at 298 K, dashed line—only noble gases; solid line—all adsorbates.

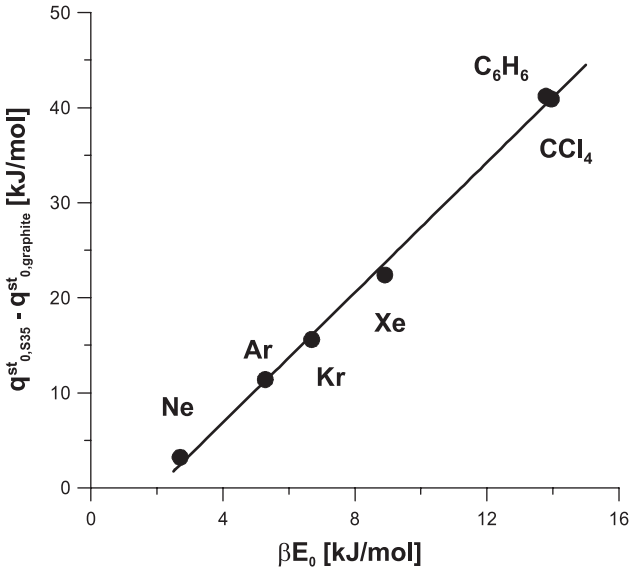

Figure 12. Recovering the correlation of Stoeckli and Morell from GCMC simulations on structure S35 and on graphite (the data for CCl_4 and C_6H_6 are for 298 K).

should expect that it should be fulfilled for systems where the dispersion interactions in the adsorbed phase dominate. The DR-plot is more sensitive to changes in the energetic or geometric parameters of adsorbed fluids if the carbon structure is more microporous; however, the deviation from linearity strongly depends on the type of studied adsorbate and the

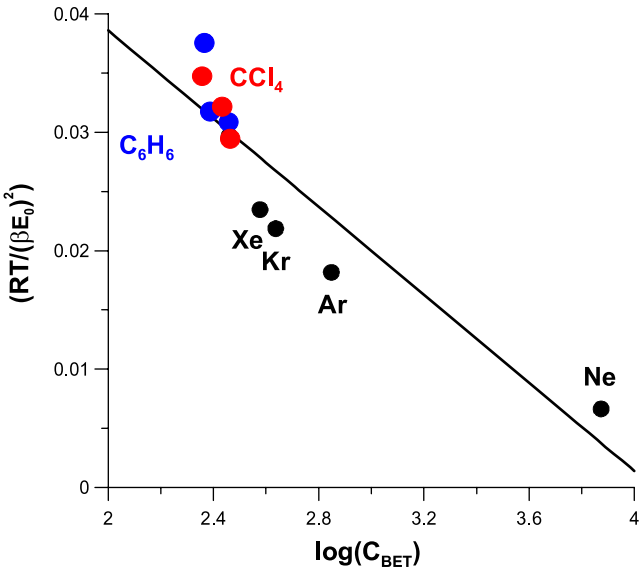

Figure 13. Recovering of the Tsunoda's correlation from simulation data on S35 structure.

temperature. For activated carbons having a wide distribution of micropores the DRS model leads to the most realistic PSD, and noble gases or carbon tetrachloride adsorption data should be applied to obtain reliable pore characteristics. On the other hand, if the studied sample is highly microporous, the JCh model should be preferred and one should apply the data of adsorption of noble gases to obtain the most realistic PSD curve. For the first case the DRS model predicts the average

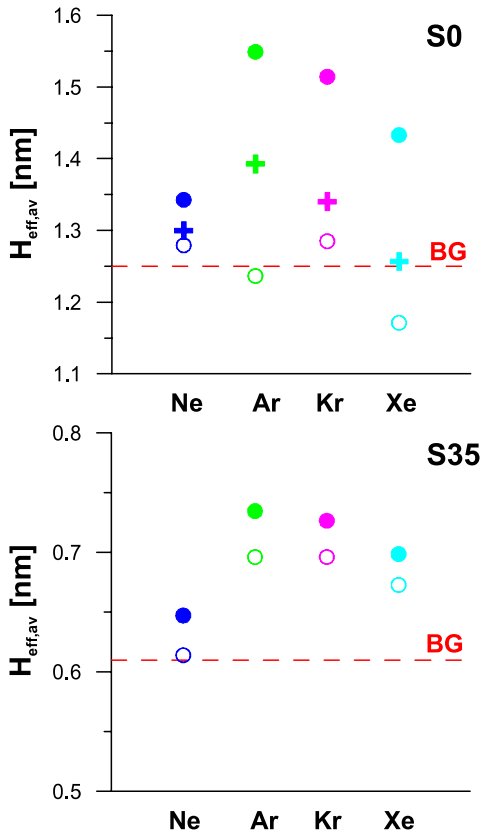

Figure 15. The comparison of the average micropore diameters from BG method wit those calculated from the JCh model (filled circles), DRS equation (open circles), and DI equation (crosses) for the both studied structures.

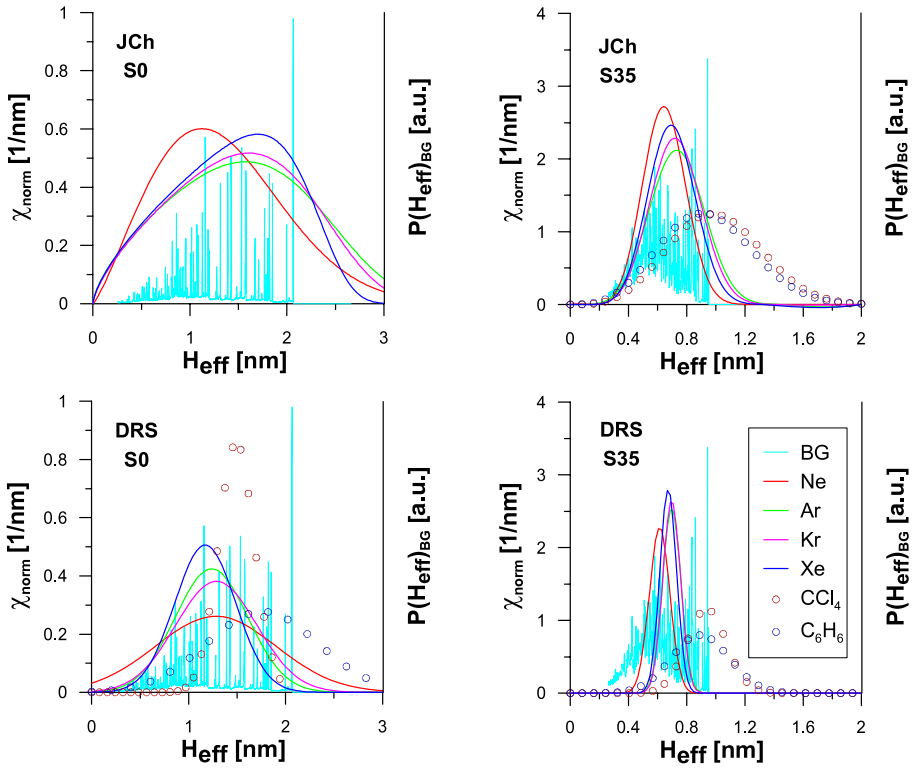

Figure 14. The comparison of the absolute pore size distributions from BG method with those obtained from DRS and JCh models; CCl_4 and C_6H_6 at 298 K.

micropore diameter well, and the best results are recorded for Ar adsorption data. On the other hand, if carbon has narrow microporosity both models can be successfully applied for the calculation of the average pore diameters based on noble gases adsorption data.

Acknowledgments

We acknowledge the use of the computer cluster at Poznań Supercomputing and Networking Center and the Information and Communication Technology Center of the Nicolaus Copernicus University (Toruń, Poland). The project was supported by grants N N204 288634 (2008–2011) and N N204 009934 (2008–2010).

References

[1] Biggs M J, Buts A and Williamson D 2004 *Langmuir* **20** 5786
[2] Biggs M J, Buts A and Williamson D 2004 *Langmuir* **20** 7123
[3] Biggs M J and Buts A 2006 *Mol. Simul.* **32** 579
[4] Biggs M J and Buts A 2002 *Proc. Carbon '02 Conf. (Beijing)* p 16
[5] Biggs M J and Buts A 2002 *Proc. AIChE Ann. Meet.* p 930
[6] Chen H and Sholl D S 2007 *Langmuir* **23** 6431
[7] Biggs M J 2001 *Proc. AIChE Ann. Meet.* p 1640
[8] Biggs M J and Buts A 2003 *Proc. AIChE Ann. Meet.* p 17
[9] Terzyk A P, Furmaniak S, Gauden P A, Harris P J F, Włoch J and Kowalczyk P 2007 *J. Phys.: Condens. Matter* **19** 406208
[10] Petersen T, Yarovsky I, Snook I, McCulloch D G and Opleteal G 2003 *Carbon* **41** 2403
[11] Pikunic J, Clinard Ch, Cohaut N, Gubbins K E, Guet J-M, Pellenq R J-M, Rannou I and Rouzaud J-N 2003 *Langmuir* **19** 8565
[12] Brennan J K, Thomson K T and Gubbins K E 2002 *Langmuir* **18** 5438
[13] Harris P J F and Tsang S C 1997 *Phil. Mag.* A **76** 667
[14] Harris P J F 1997 *Int. Mater. Rev.* **42** 206
[15] Harris P J F 2005 *Crit. Rev. Solid State Mater. Sci.* **30** 235
[16] Terzyk A P, Furmaniak S, Harris P J F, Gauden P A, Włoch J, Kowalczyk P and Rychlicki G 2007 *Phys. Chem. Chem. Phys.* **9** 5919
[17] Stoeckli F 2001 *Russ. Chem. Bull.* **50** 2265
[18] Linares-Solano A, Martin-Gullon I, Salinas-Martínez de Lecea C and Serrano-Talavera B 2000 *Fuel* **79** 635
[19] Carrasco-Marin F, Alvarez-Merino M A and Moreno-Castilla C 1996 *Fuel* **75** 966
[20] Carrasco-Marin F, Lopez-Ramon M V and Moreno-Castilla C 1993 *Langmuir* **27** 85
[21] Kakei K, Ozeki S, Suzuki T and Kaneko K 1990 *J. Chem. Soc. Faraday Trans.* **86** 371
[22] Marsh H 1987 *Carbon* **25** 49
[23] Ozawa S, Kusumi S and Ogino Y 1976 *J. Colloid Interface Sci.* **56** 83
[24] Jaroniec M and Madey R 1991 *Langmuir* **7** 173
[25] Aoshima M, Fukasawa K and Kaneko K 2000 *J. Colloid Interface Sci.* **222** 179
[26] Ismadij S and Bhatia S K 2000 *Langmuir* **16** 9303
[27] Nieszporek K 2002 *Pol. J. Chem.* **76** 1447
[28] Serpinski V V and Jakubov T S 1993 *Adsorpt. Sci. Technol.* **10** 85
[29] Jaroniec M 1975 *Surf. Sci.* **50** 553
[30] Ustinov E A, Polyakov N S and Petukhova G A 1999 *Russ. Chem. Bull.* **48** 261
[31] Chen S G and Yang R T 1996 *J. Colloid Interface Sci.* **177** 298
[32] Chen S G and Yang R T 1994 *Langmuir* **10** 4244
[33] Dobruskin V K 1998 *Langmuir* **14** 3840
[34] Terzyk A P and Gauden P A 2001 *Colloids Surf.* A **177** 57
[35] Terzyk A P, Gauden P A, Zawadzki J, Rychlicki G, Wiśniewski M and Kowalczyk P 2001 *J. Colloid Interface Sci.* **243** 183
[36] Gauden P A, Terzyk A P, Rychlicki G, Kowalczyk P, Ćwiertnia M S and Garbacz J K 2004 *J. Colloid Interface Sci.* **273** 39
[37] Terzyk A P, Gauden P A and Kowalczyk P 2002 *Carbon* **40** 2879
[38] Dubinin M M, Neimark A V and Serpinski V V 1993 *Carbon* **31** 1015
[39] Rudziński W, Nieszporek K and Dąbrowski A 1993 *Adsorpt. Sci. Technol.* **10** 35
[40] Rudziński W, Nieszporek K, Cases J M, Michot L I and Villeras F 1996 *Langmuir* **12** 170
[41] Tovbin Yu 1998 *Russ. Chem. Bull.* **47** 637
[42] Samios S, Stubos A K, Kanellopoulos N K, Cracknell R F, Papadopoulos G K and Nicholson D 1997 *Langmuir* **13** 2795
[43] Ohba T, Suzuki T and Kaneko K 2000 *Carbon* **38** 1879
[44] Ohba T and Kaneko K 2001 *Langmuir* **17** 3666
[45] El-Merraouni M, Aoshima M and Kaneko K 2000 *Langmuir* **16** 4300
[46] Nguyen C and Do D D 2001 *Carbon* **39** 1327
[47] Aranovich G L and Donohue M 1995 *Carbon* **33** 1369
[48] Dubinin M M and Astakhov V A 1971 *Izv. Akad. NaukSSR, Ser. Khim.* **1** 5
[49] Nakahara K T, Hirata M and Ohmori T 1975 *J. Chem. Eng. Data* **20** 195
[50] Zukal A and Kadlec O 1973 *Coll. Czech. Chem. Commun.* **38** 321
[51] Lopez-Ramon M V, Stoeckli F, Moreno-Castilla C and Carrasco-Martin F 2000 *Langmuir* **16** 5967
[52] Pons M and Grenier Ph 1986 *Carbon* **24** 615
[53] Bakaev V A and Steele W A 1993 *Adsorpt. Sci. Technol.* **10** 123
[54] Bakaev V A 1988 *Surf. Sci.* **198** 571
[55] Izotova T I and Dubinin M M 1965 *Zh. Fiz. Chim.* **39** 2796
[56] Dubinin M M and Plavnik G M 1968 *Carbon* **6** 183
[57] Domingo-Garcia M, Fernandez-Morales I, Lopez-Garzon F J and Moreno-Castilla C 1997 *Langmuir* **13** 1218
[58] Stoeckli H F 1986 *J. Colloid Interface Sci.* **59** 521
[59] Jaroniec M and Choma J 1986 *Mater. Chem. Phys.* **15** 521
[60] Dubinin M M 1989 *Carbon* **27** 457
[61] Kowalczyk P, Gauden P A, Terzyk A P, Do D D and Rychlicki G 2002 *Ann. UMCS Sect. AA, Chemia* **58** 46
[62] Bhattacharya S and Gubbins K E 2006 *Langmuir* **22** 7726
[63] Humphrey W, Dalke A and Schulten K 1996 *J. Mol. Graph.* **14** 33 http://www.ks.uiuc.edu/Research/vmd/
[64] Do D D and Do H D 2005 *Fluid Phase Equilib.* **236** 169
[65] Do D D and Do H D 2006 *J. Phys. Chem.* B **110** 9520
[66] Ungerer P, Travitian B and Boutin A 2005 *Application of Molecular Simulation in the Oil and Gas Industry* (Paris: Editions Technip)
[67] Frenkel D and Smit B 1996 *Understanding Molecular Simulation* (San Diego: Academic)
[68] Stoeckli F and Morell D 1980 *Chimia* **12** 502
[69] Storn R and Price K 1997 *J. Glob. Optim.* **11** 341 http://www.icsi.berkeley.edu/~storn/code.html
[70] Furmaniak S, Gauden P A, Terzyk A P and Rychlicki G 2008 *Adv. Colloid Interface Sci.* **137** 82
[71] Wood G O 2001 *Carbon* **39** 343
[72] Wojsz R 1989 *Characteristics of the Structural and Energetic Heterogeneity of Microporous Carbon Adsorbents Regarding the Adsorption of Polar Substances* (Toruń: UMK) (in Polish)
[73] Terzyk A P, Gauden P A and Kowalczyk P 2002 *J. Colloid Interface Sci.* **254** 242

[74] Jaroniec M, Lu X and Madey R 1991 *Monatsh. Chem.* **122** 577
[75] Gauden P A and Terzyk A P 2000 *J. Colloid Interface Sci.* **227** 482
[76] Gauden P A, Terzyk A P, Rychlicki G and Kowalczyk P 2001 *J. Colloid Interface Sci.* **244** 439
[77] Rychlicki G and Terzyk A P 1998 *Adsorpt. Sci. Technol.* **16** 641
[78] Tsunoda R 1987 *J. Colloid Interface Sci.* **117** 291
[79] Rudziński W and Everett D H 1992 *Adsorption of Gases on Heterogeneous Surfaces* (London: Academic)